THE JOURNAL OF BIOLOGICAL CHEMISTRY
Vol. 277, No. 15, Issue of April 12, pp. 13257–13267, 2002

Printed in U.S.A.

Involvement of a Nine-residue Loop of Streptokinase in the Generation of Macromolecular Substrate Specificity by the Activator Complex through Interaction with Substrate Kringle Domains*

Received for publication, August 31, 2001, and in revised form, January 28, 2002
Published, JBC Papers in Press, January 30, 2002, DOI 10.1074/jbc.M108422200

Jayeeta Dhar‡, Abhay H. Pande‡, Vasudha Sundram, Jagpreet S. Nanda, Shekhar C. Mande, and Girish Sahni§

From the Institute of Microbial Technology, Sector 39-A, Chandigarh-160036, India

The selective deletion of a discrete surface-exposed epitope (residues 254–262; 250-loop) in the β domain of streptokinase (SK) significantly decreased the rates of substrate human plasminogen (HPG) activation by the mutant ($SK_{del254–262}$). A kinetic analysis of $SK_{del254–262}$ revealed that its low HPG activator activity arose from a 5–6-fold increase in K_m for HPG as substrate, with little alteration in k_{cat} rates. This increase in the K_m for the macromolecular substrate was proportional to a similar decrease in the binding affinity for substrate HPG as observed in a new resonant mirror-based assay for the real-time kinetic analysis of the docking of substrate HPG onto preformed binary complex. In contrast, studies on the interaction of the two proteins with microplasminogen showed no difference between the rates of activation of microplasminogen under conditions where HPG was activated differentially by nSK and $SK_{del254–262}$. The involvement of kringles was further indicated by a hypersusceptibility of the $SK_{del254–262}$·plasmin activator complex to ε-aminocaproic acid-mediated inhibition of substrate HPG activation in comparison with that of the nSK·plasmin activator complex. Further, ternary binding experiments on the resonant mirror showed that the binding affinity of kringles 1–5 of HPG to $SK_{del254–262}$·HPG was reduced by about 3-fold in comparison with that of nSK·HPG. Overall, these observations identify the 250 loop in the β domain of SK as an important structural determinant of the inordinately stringent substrate specificity of the SK·HPG activator complex and demonstrate that it promotes the binding of substrate HPG to the activator via the kringle(s) during the HPG activation process.

Streptokinase (SK),[1] a bacterial protein secreted by the Lancefield Group C β-hemolytic streptococci, is widely used as a thrombolytic agent in the treatment of various circulatory disorders, including myocardial infarction (1). Unlike other human plasminogen (HPG) activators, like tissue plasminogen activator and urokinase, SK does not possess any intrinsic enzymatic activity. Instead, SK forms an equimolar, stoichiometric complex with "partner" HPG or plasmin (HPN), which then catalytically activates free "substrate" molecules of HPG to HPN by selective cleavage of the Arg^{561}-Val^{562} peptide bond (2, 3). It is believed that consequent to the initial SK·HPG complexation, there is a structural rearrangement within the complex, and even before any proteolytic cleavage takes place, an active center within the HPG moiety capable of undergoing acylation is formed (3). This activated complex is rapidly transformed into an SK·HPN complex and develops an HPG activator activity. Unlike free HPN, however, which is essentially a trypsin-like protease with broad substrate preference, SK·HPN displays a very narrow substrate specificity (4). The structural basis of the conversion of the broadly specific serine protease HPN to a highly substrate-specific protease, once complexed with the "cofactor" SK, with exclusive propensity for acting on the target scissile peptide bond in HPG has been the subject of active investigations with both fundamental and applied implications (5–12).

SK has been shown to be composed of three structurally similar domains (termed α, β, and γ), separated by random coils and small, flexible regions at the amino and carboxyl termini (5, 7, 8). The recently solved crystal structure of the catalytic domain of HPN complexed with SK strongly indicates how SK might modulate the substrate specificity of HPN by providing a "valley" or cleft in which the macromolecular substrate can dock through protein-protein interactions, thus positioning the scissile peptide bond optimally for cleavage by the HPN active site, thereby conferring a narrow substrate preference onto an otherwise "indiscriminate" active center. In this structure, SK does not appear to induce any significant conformational changes in the active site residues directly but, along with partner HPG, seems to provide a template on which the substrate molecule can dock through protein-protein interactions, resulting in the optimized presentation of the HPG activation loop at the active center of the complex (6, 8). However, the identity of these interactions and their contributions to the formation of the enzyme-substrate intermediate(s) remains a mystery so far.

Besides the well recognized "switch" in substrate preference (4), the binding of SK to HPN results in a severalfold enhancement of the K_m for diverse small molecular weight chromogenic peptide substrates but relatively little alteration in their k_{cat} values as compared with free HPN, indicating that the pri-

* This work was supported by grants from the Department of Biotechnology and the Council of Scientific and Industrial Research, Government of India. The costs of publication of this article were defrayed in part by the payment of page charges. This article must therefore be hereby marked "*advertisement*" in accordance with 18 U.S.C. Section 1734 solely to indicate this fact.

‡ These two authors have contributed equally to this work.

§ To whom correspondence should be addressed: Inst. of Microbial Technology, Sector 39-A, Chandigarh-160036, India. Tel.: 91-172-695215; Fax: 91-172-690585; E-mail: sahni@imtech.res.in.

[1] The abbreviations used are: SK, streptokinase; PG, plasminogen (irrespective of source); HPG, human plasminogen; HPN, human plasmin; μPN, microplasmin; μPG, microplasminogen; K1–5, kringles 1–5 of plasminogen; NPGB, *p*-nitrophenyl *p*-guanidinobenzoate; SOE, splicing-overlap-extension; EACA, ε-amino caproic acid; nSK, native-like SK.

mary, covalent specificity characteristics of the active center of HPN upon SK binding are unchanged but result in steric hindrance/reduced accessibility for even the small molecular weight peptide substrates. Thus, the remarkable alteration of the macromolecular substrate specificity of HPN by SK is currently thought to be due to "exosites" generated on the SK·HPN complex, as shown recently by the elegant use of active site-labeled fluorescent HPN derivatives (10). Peptide walking studies in our laboratory had also indicated that short peptides based on the primary structure of SK, particularly those derived from selected regions in the α and β domains, displayed competitive inhibition for HPG activation by the preformed SK·HPN complex under conditions where the 1:1 complexation of SK and HPN was essentially unaffected (11, 12) However, the crystal structure of SK complexed with microplasmin(ogen) (8), while providing a high degree of resolution of the residues involved in the SK·μPN complexation, yielded few unambiguous insights regarding the interactions engendered between the activator complex and substrate HPG. This is probably due to the binary nature of the complex (*i.e.* an absence of a juxtaposed substrate molecule, large average thermal factors especially in the β domain, and a total absence, in both partner and substrate HPG, of the kringles that are known to be important in HPG activation) (13). Thus, despite a detailed and high resolution exposition of the overall nature of protein-protein interactions in the SK·μPN binary complex, discrete structures/epitopes of SK, if any, that are directly involved in the exosite formation process by the full-length activator complex have not yet been identified.

Previously, charged side chains, both in HPG, particularly around the active center (14), and in SK in the β domain (16, 17), have been shown to be important for HPG activation ability. However, a clear cut identification of a structural epitope/element in conferring substrate HPG affinity onto the SK·PG activator complex has not been demonstrated until now. Of the three domains of SK, the central β domain displays maximal affinity for HPG (15), the N-terminal α domain displays relatively lesser affinity for HPG with the γ domain showing much less affinity of for HPG.[2] Solution and structural studies suggest that both α and β domains are involved in the substrate recognition phenomenon (8, 12). Mutagenesis studies have also implicated positively charged residues in the β domain to be important but have failed to show that these residues are directly involved in substrate recognition by the binary complex (17). An examination of the crystal structure of the free β domain (18) and its comparison with the other two SK domains possessing closely similar (but not identical) structures revealed the presence of a distinct flexible loop in the β domain (the 250-loop) that protrudes into the solvent (Fig. 1).

In the present study, we chose to delete this loop based on the premise that if this structural motif is involved in substrate recognition, discrete deletion of this loop would lead to a selective increase in K_m of the activator complex. The results obtained provide clear cut evidence of the role played by this nine-residue loop in substrate recognition and thus identify a functionally important component of the macromolecular substrate-specific exosite operative in the SK·HPN complex, which interacts via the kringle(s) in HPG.

EXPERIMENTAL PROCEDURES

Reagents

Glu-plasminogen was either purchased from Roche Diagnostics Inc. or purified from human plasma by affinity chromatography (19). The RNA polymerase promoter-based expression vector, pET23(d) and *Escherichia coli* strain BL21 (DE3) were products of Novagen Inc. (Madison, WI). Thermostable DNA polymerase (*pfu*) was obtained from Stratagene Inc. (La Jolla, CA), and restriction endonucleases, T4 DNA ligase, and other DNA-modifying enzymes were acquired from New England Biolabs (Beverly, MA). Oligonucleotide primers were supplied by Integrated DNA Technologies Inc., (Indianapolis, IN). HPN was prepared by digesting Glu-HPG with urokinase covalently immobilized on agarose beads using a ratio of 300 Plough units/mg HPG in 50 mM Tris-Cl, pH 8.0, 25% glycerol, and 25 mM L-lysine at 22 °C for 10 h (15, 16). All other reagents were of the highest analytical grade available.

Design and Construction of $SK_{del254–262}$ and $\beta_{wild\ type}/\beta_{del254–262}$

A set of mutagenic and flanking primers, carrying unique restriction sites, were used in polymerase chain reactions to generate DNA fragments having overlapping ends. Thereafter, splicing-overlap-extension PCR (SOE-PCR) reactions (20) were carried out, resulting in amplification products, which were cloned in the pET23(d) expression vector (16, 21).

Oligonucleotide primers for SOE-PCR for the construction of $SK_{del254–262}$ were as follows. The mutagenic primers were as follows: upstream primer, 5′-AACAGGCTTATAGGGAAATAAACAACACTGACCTGATATCTGAGAAA-3′; downstream primer, 5′ TGTTGTTTATTTCCCTATAAGCCTGTTCCCGATTTTTAA 3′. The flanking primers were as follows: upstream primer, 5′-ATTTATGAACGTGACTCCTCAATCGTC-3′; downstream primer, 5′-ATAGGCTAAATGATAGCTAGCATTCTCTCC-3′.

Oligonucleotide primers for SOE-PCR for the construction of $\beta_{wild\ type}$ and $\beta_{del254–262}$ were as follows. Sequences of the mutagenic primers were as follows: upstream primer, 5′-AACAGGCTTATAGGGAAATAAACAACACTGACCTGATATCTGAGAAA-3′; downstream primer, 5′-TGTTGTTTATTTCCCTATAAGCCTGTTCCCGATTTTTAA-3′. Sequences of the flanking primers were as follows: upstream primer, 5′-GTGGAATATACTGTACAGTTTACTCC-3′; downstream primer, 5′-ATCGGGATCCTATTTCAAGTGACTGCGATCAAAGGG-3′.

Expression and Purification of nSK/$SK_{del254–262}$

Both proteins were expressed intracellularly in *E. coli* BL21 (DE3) cells after induction with isopropyl-1-thio-β-D-galactopyranoside essentially according to the instructions of the supplier (Novagen Inc.). The host-vector system for the expression of the cDNA corresponding to mature SK from *Streptococcus equisimilis* H46A after in-frame juxtaposition of an initiator methionine codon (so as to express the protein as Met-SK) has been described earlier (16). However, protein sequence analysis of the purified SK expressed intracellularly in *E. coli* (referred to as nSK hereafter) was found to have its N-terminal Met removed at a 50% level. The same case was seen in the mutant ($SK_{del254–262}$) prepared similarly from *E. coli* employing the same expression vector. The pelleted cells were sonicated, and the proteins in the supernatants were precipitated with ammonium sulfate (16). This fraction, after dissolution in 20 mM Tris-Cl buffer, pH 7.5, was then chromatographed on a Poros-D anion exchange column fitted onto a Bio-Cad Sprint liquid chromatographic workstation (Perseptive Biosystems Inc., Framingham, MA). nSK/$SK_{del254–262}$ were eluted using a linear gradient of NaCl (0–0.5 M) in 20 mM Tris-Cl buffer, pH 7.5. The eluted proteins were more than 95% pure, as analyzed by SDS-PAGE.

Expression and Purification of $\beta_{wild\ type}/\beta_{del254–262}$

Both proteins were expressed intracellularly in *E. coli* BL21 (DE3) cells as inclusion bodies. The pellet obtained after sonication was taken up in 8 M urea and placed under gentle shaking conditions for 30 min to effect dissolution. After a high speed centrifugation step, the protein in the supernatant was refolded by 20-fold dilution with 20 mM Tris-Cl buffer, pH 7.5. The β domain was then purified to more than 95% homogeneity by chromatography on DEAE-Sepharose Fast-flow (Amersham Biosciences) at 4 °C using a linear NaCl gradient (0–0.25 M NaCl in 20 mM Tris-Cl buffer, pH 7.5).

Preparation of μPG and K1–5

Microplasminogen, the catalytic domain of plasminogen (residues Lys^{530}–Asn^{790}) devoid of all kringles was prepared by cleavage of HPG by HPN under alkaline conditions (0.1 N glycine/NaOH buffer, pH 10.5) at 25 °C. Microplasminogen was purified from the reaction mixture by passing through a Lys-Sepharose column (Amersham Biosciences), followed by a soybean-trypsin inhibitor-Sepharose 4B column to absorb HPN and μPN, as reported (22). The flow-through

[2] V. Sundram, K. Rajagopal, A. Chaudhary, S. S. Komath, and G. Sahni, unpublished observations.

was then subjected to molecular sieve chromatography, after concentration by ultrafiltration, on a column (16 × 60 cm) of Superdex-75™ (Amersham Biosciences). The purity of μPG formed was analyzed by SDS-PAGE, which showed a single band moving at the position expected from its molecular size (22). The proteolytic fragment containing all of the HPG kringle domains (K1–5) was prepared by incubating HPG with urokinase-free HPN (5:1 ratio of HPG and HPN) under alkaline conditions (0.1 N glycine/NaOH, pH 9.0) for 72 h at 25 °C. Under these conditions, the proteolytic conversion of native HPG to K1–5 was found to be quantitative, with minimal residual HPG. HPN was removed from the reaction mixture by passing through a soybean trypsin inhibitor-Sepharose column (1.6 × 3.6 cm). This was followed by gel filtration on Superdex-75, to obtain HPG- and μPG-free K1–5. The purity of this preparation was confirmed by SDS-PAGE analysis (23). Activation with urokinase, which is known to be a good activator of μPG irrespective of the presence of kringle domains (22), was used to establish that the activation of this preparation, when used as substrate, was comparable with that obtained when using SK·HPN as the activator species.

Characterization of $SK_{del254-262}$

Amidolytic Activation of Equimolar HPG-nSK/$SK^{del254-262}$ Complexes—Aliquots (50 nM) were withdrawn from equimolar HPG·nSK/$SK_{del254-262}$ complexes at regular periods and transferred to a 100-μl quartz microcuvette containing 2 mM tosyl-glycyl-prolyl-lysine-4-nitranilide-acetate (Chromozym® PL) and 50 mM Tris-Cl, pH 7.5, at 22 °C. The change in absorbance at 405 nm was monitored to compute the kinetics of amidolytic activation (12, 24).

Esterolytic Activation of Equimolar HPG·nSK/$SK_{del254-262}$ Complexes—Five μM HPG was added to an assay cuvette containing 5.5 μM nSK/$SK_{del254-262}$, 100 μM NPGB, and 10 mM phosphate buffer, pH 7.5, and the "burst" of *p*-nitrophenol release was monitored at 410 nm as a function of time at 22 °C (3, 25).

Determination of Kinetic Constants for HPG Activator Activity of nSK/$SK_{del254-262}$—Varying amounts of HPG were added to the assay cuvette containing fixed amounts of nSK/$SK_{del254-262}$ and chromogenic substrate (1 mM), and the change in absorbance was monitored at 405 nm as a function of time at 22 °C. Also, the kinetics of HPG activation by HPN·nSK/$SK_{del254-262}$ complexes were measured by transferring suitable aliquots of preformed HPN·nSK/$SK_{del254-262}$ complexes to the assay cuvette containing different concentrations of substrate HPG (24). To compute the k_{cat}, the number of HPN active sites was determined using the NPGB reaction (3, 25, 26).

Assay for the Determination of the Steady-state Kinetic Constants for Amidolytic Activity of nSK/$SK_{del254-262}$—nSK/$SK_{del254-262}$ and HPN were precomplexed at 4 °C in equimolar ratios (100 nM each) for 1 min in 50 mM Tris-Cl, pH 7.5, containing 0.5% bovine serum albumin, and an aliquot of the reaction mixture was transferred to a 100-μl assay cuvette containing 50 mM Tris-Cl buffer, pH 7.5, and varying concentrations of the chromogenic substrate (0.1–2 mM) to obtain a final concentration of 10 nM complex in the reaction. The reaction was monitored spectrophotometrically at 405 nm for 5 min at 22 °C. The kinetic constants were calculated by standard methods (25).

Kinetic Analysis of Protein-Protein Interactions Using Resonant Mirror Technology

Binary Interaction Analysis—Association and dissociation between HPG and the nSK/$SK_{del254-262}$, referred to hereafter as binary interaction, were followed in real time by resonant mirror-based detection using the IAsys Plus™ system (Cambridge, UK) (27, 28). In these experiments, streptavidin was captured on biotin cuvette according to the manufacturer's protocols (IAsys protocol 1.1). This was followed by the attachment of (mildly) biotinylated HPG to the streptavidin captured on the cuvette. Nonspecifically bound HPG was then removed by repeated washing with phosphate-buffered saline followed by three washes with 10 mM HCl. The net response chosen for the immobilized biotinylated HPG onto the cuvette was 700–800 arc seconds in all experiments. Experiments were performed at 25 °C in 10 mM phosphate-buffered saline, pH 7.4, containing 0.05% Tween 20 and 5×10^{-3} M NPGB (binding buffer). The latter was included in order to prevent plasmin-mediated proteolysis.

After equilibrating the cuvette with binding buffer, varying concentrations of either nSK or $SK_{del254-262}$ were added, and each binding response was monitored during the "association" phase. Subsequently, the cuvette was washed with binding buffer, and the "dissociation" phase was recorded (29). Following each cycle of analysis, the cuvette was regenerated by washing with 10 mM HCl, and base line was reestablished with binding buffer. In parallel, in the control cell in the dual channel cuvette, immobilized streptavidin alone was taken as a negative control for the binding studies. In experiments where EACA was used to examine its effect on SK-HPG interaction, the binary complex was formed between ligate nSK/$SK_{del254-262}$ and immobilized HPG in binding buffer (as described above). The dissociation of the binary complexes was done by washing the cuvette with EACA instead of buffer alone.

The data were analyzed after subtraction of the corresponding nonspecific refractive index component(s), and the kinetic constants were calculated from the sensorgrams by nonlinear fitting of the association and dissociation curves according to 1:1 model $A + B = AB$ using the software FASTfit™, supplied by the manufacturers. Briefly, the association curves at each concentration of ligate were fitted to the pseudo-first order equation to calculate the observed rate constant (k_{on}). Then the concentration dependence of k_{on} was fitted using linear regression to find the association rate constant (k_a) from the slope of the linear fit (30). The dissociation rate constant (k_d) was calculated from the average of four dissociation curves obtained at saturating concentration of ligate. The equilibrium dissociation constant (K_D) was then calculated as k_d/k_a. Values of K_D obtained using this relationship were in good approximation to those obtained by Scatchard analysis of the extent of association (data not shown).

Ternary Interaction Analysis—Resonant mirror technology-based biosensor was also used to measure the rate and equilibrium dissociation constants describing interactions between soluble ligate (PG, μPG, or K1–5) and nSK/SKdel$_{254-262}$ complexed with immobilized HPG, a situation simulating substrate binding to binary complex and hereafter referred to as ternary interaction. In binary interaction studies, it was evident that when soluble nSK/$SK_{del254-262}$ was added to immobilized HPG, a rapid and avid SK·HPG binary complex formation occurs. The dissociation of this complex is very slow due to the high stability of the SK·HPG complex, as has been observed by others also (15). After allowing the complex to dissociate maximally (~20 min), the dissociation base line becomes stable, which remains unaffected even after washing with 2.5 mM EACA. It has been reported that when SK was preincubated with immobilized HPG, EACA was >100-fold less potent at dissociating the binary complex than it was at preventing binary complex formation when SK and EACA were added synchronously to immobilized HPG (13). Thus, this comparative resistance to dissociation of the SK·HPG binary complex by EACA permitted us to study ternary substrate interaction under conditions that did not adversely affect the stability of the binary interaction. In contrast, EACA was found to be strongly inhibitory to ternary complex formation (see below).

In a typical ternary interaction experiment, a stable binary complex was formed by adding a saturating amount of either nSK or $SK_{del254-262}$ onto HPG, immobilized on streptavidin captured on biotin cuvette. After maximally dissociating the binary complex with binding buffer and washing with 2.5 mM EACA, a stable dissociation base line was obtained. Varying concentrations of either "ternary" HPG (0.1–1.0 μM), μPG (1–6 μM), or K1–5 (1–6 μM) were then added to monitor the binding by recording the association phase. Subsequently, the cuvette was washed with binding buffer three times, and the dissociation phase was recorded. After each cycle of analysis, the original base line was reestablished by stripping off the undissociated ternary ligate with 2.5 mM EACA followed by three washes with binding buffer. It was established that EACA, at this concentration, completely abolishes the interaction of ternary HPG with the binary complex, while the binary complex remains stable. The latter attribute was considered to be a necessary precondition to obtain reliable and reproducible values of the kinetic constants for ternary complex formation and dissociation. In order to test whether this was indeed so, control experiments were carried out in which the ternary complex formation and dissociation experiments were done at various time intervals after a stable base line was attained subsequent to binary complex formation followed by buffer and EACA washes, as described above. It was observed that the rate constants so obtained did not differ significantly (within a margin of ±5%) as a function of time. In experiments where μPG was used as soluble ternary ligate, 1 mM EACA was found to be sufficient to strip off the undissociated μPG, whereas washing with binding buffer alone resulted in incomplete regeneration of base line. Association and dissociation phases at varying ligate (HPG, μPG and K1–5) concentrations were fitted as described above, and the equilibrium dissociation constant/s were calculated as k_d/k_a.

The effect of EACA on the binding of soluble ternary HPG to nSK/$SK_{del254-262}$ complexed with immobilized HPG was assessed by measuring the binding extents, measured in arc second units, at equilibrium at a fixed concentration of substrate HPG (0.4 μM) in the

presence of varying EACA concentrations (0–2 mM). For the analysis of these data, the binding extent in buffer alone was taken as 100%, and varying extents of formation of ternary complexes at equilibrium were plotted as a function of EACA concentration to obtain EACA-dependent binding isotherms for nSK and $SK_{del254-262}$. As controls, the effect of EACA was similarly examined for dissociation of preformed complexes between HPG and either nSK or $SK_{del254-262}$ in the absence of substrate HPG.

Circular Dichroic Analysis of nSK/$SK_{del254-262}$

Far-UV CD spectra of proteins (concentration 0.15 mg/ml in phosphate-buffered saline, pH 7.2) were recorded on a Jasco-720 spectropolarimeter. Measurements were carried out from 200 to 250 nm in a 0.1-cm path length cell, and the appropriate buffer base line was subtracted from the protein spectra. The final spectrum analyzed was an average of 10 scans (31).

Modeling Studies

Cartesian coordinates of the kringle 5 domain of HPG (used as a prototypical representative structure of HPG kringle domains) and those of SK β domain and the SK-μPN complex were retrieved from the Protein Data Bank (codes 5HPG, 1C4P, and 1BML, respectively). The β domain in SK-μPN reveals several disordered loops, including the 250-loop (8). The coordinates in this complex were hence replaced with those of the isolated β domain (18). The isolated β domain was superimposed on the β domain of the complex, and the corresponding set of coordinates was simply replaced. The isolated β domain has the 250-loop clearly defined; hence, it is more suitable for docking analysis.

Molecular surface for a typical HPG kringle domain was generated using the kringle 5 coordinates (taken as a prototype) with the aid of GRASP (32) with standard atomic radii, and the probe radius of 1.4 Å. Electrostatic potential was then mapped onto the molecular surface. There are two distinct regions of negative charges on the surface. The negatively charged surface of kringles is likely to interact with the positively charged loop of the SK structure, and therefore these regions were of particular interest in generating the SK β-μPN-kringle docked complex. One of the negatively charged regions is at the interface of the dimeric kringle structure. This region was therefore not considered appropriate for docking. The other negatively charged region was then manually brought into close proximity of the 250-loop of SK β domain. The best docked complex is shown in Fig. 7. Remarkably, the surface of the kringle showed nearly perfect complementarity to the surface of the SK-μPN complex. The mode of docking also revealed that the C terminus of the kringle domain is within connecting distance of the N terminus of the μPN moiety, as would be expected in the physiological situation. Thus, the close complementarity of kringle and SK-μPN surfaces, the perfect electrostatic match among the two structures, and the proximity between connecting peptide units suggest that indeed the kringle might dock onto SK-μPN in the mode shown in Fig. 7.

RESULTS AND DISCUSSION

To investigate the functional role of the 250-loop (*viz*. its involvement in the modulation of substrate specificity of HPN by SK), we prepared a deletion mutant ($SK_{del254-262}$) employing the SOE-PCR method (20). The desired deletion mutation was confirmed by sequencing of both strands of the cloned DNA (see "Experimental Procedures" for other details). This was followed by subcloning of the PCR amplification product in a T7 RNA polymerase promoter-based expression vector (21). With the nine-residue deletion, we expected that a minimal perturbation of the underlying β sheet would occur (Fig. 1), since the two residues flanking the loop (Tyr^{252} and Glu^{263}) had a distance of 4 Å between the C^{α} atoms (18). The *E. coli* BL21 (DE3) cells carrying the plasmid were grown in shake flasks to midlog phase, and the expression of the protein of interest was then induced by the addition of isopropyl-1-thio-β-D-galactopyranoside. $SK_{del254-262}$ was then purified from the intracellular milieu to homogeneity using a rapid, two-step protocol (16). When purified $SK_{del254-262}$ was examined for its ability to activate substrate HPG, it showed a specific activity that was only about 20% that of native-like SK (termed nSK) similarly expressed and purified using the same expression plasmid and host system.

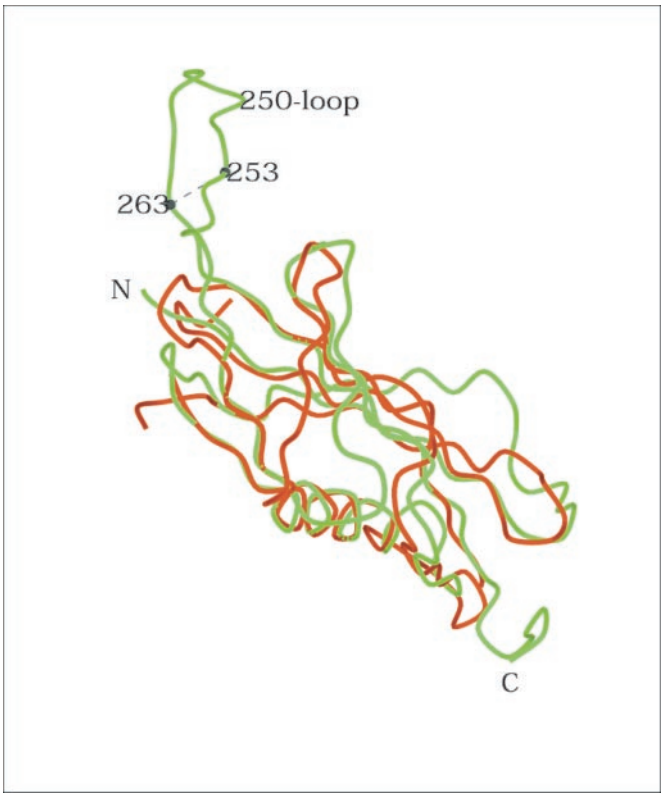

FIG. 1. **Superposition of α and β domains of streptokinase.** The β domain is shown in *green*, and the α domain is in *red*. The 250-loop is a distinct feature of the β domain, while the rest of the structure between the two domains overlaps extensively. The superposition with the γ domain of SK showed similar results (not shown). The residues 253 and 263, where the loop was truncated, are indicated.

We checked whether the deletion of the 250-loop resulted in changes in the overall folding characteristics of SK as judged by its secondary structure analyzed by CD. The far-UV CD spectra of nSK and the mutant ($SK_{del254-262}$), however, did not show any significant discernible differences (data not shown). However, since a native-like CD spectrum of the mutant could still result if relatively small, local conformational changes occurred in and around the site of the deletion in the β domain that might get "averaged out" in the presence of the CD contributions from rest of the two domains of SK in the full-length molecule, we carried out a deletion at the same site in a truncated gene encoding for the isolated β domain. The cDNAs encoding for the β domain alone and $\beta_{del254-262}$ were then expressed in *E. coli* and purified (see "Experimental Procedures" for details), and their far-UV CD spectra were recorded. Interestingly, no noticeable changes were observed in the secondary structure of $\beta_{del254-262}$ with respect to $\beta_{wild\ type}$ similarly expressed in *E. coli* also (data not shown), indicating that neither the overall secondary structure of SK nor that of the β domain alone had been perturbed by the deletion of the nine-residue loop from the protein.

To explore whether the deletion of the 250-loop resulted in any significant alteration in the affinity of the mutant with partner HPG, the kinetics of interaction between immobilized HPG and nSK were compared with those of $SK_{del254-262}$ by the resonant mirror approach using a semiautomated instrument for measuring protein-protein interactions in real time (IAsys, Cambridge UK). To examine the effect of immobilization chemistry on the values of kinetic constants, preliminary experiments were performed by immobilizing either nSK or $SK_{del254-262}$ onto carboxymethyldextran cuvettes, using an

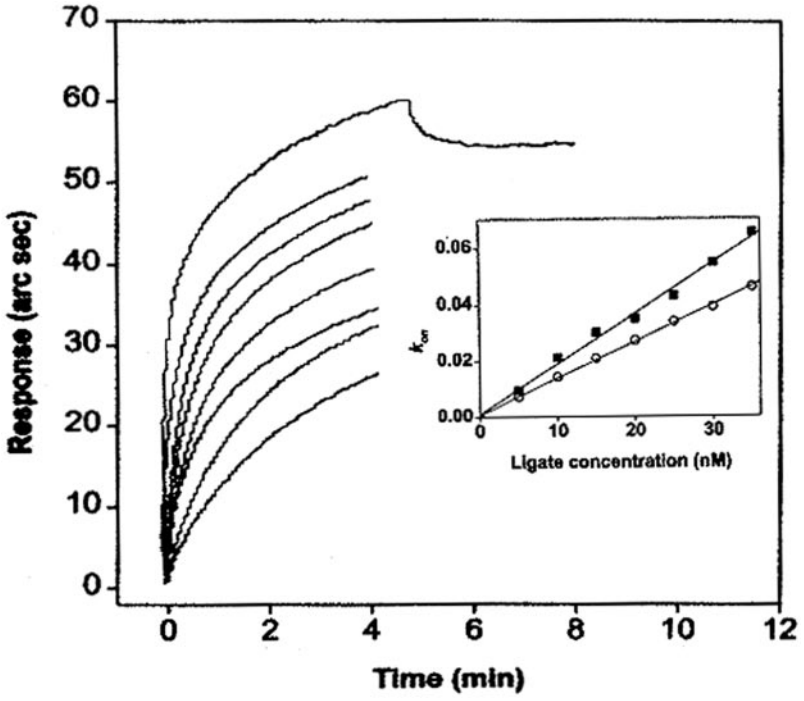

FIG. 2. **Optical biosensor determination of binding constants for the interaction of nSK/$SK_{del254–262}$ with immobilized HPG.** Overlay plots representing the binding and dissociation of nSK to the immobilized HPG are depicted. Human PG was biotinylated and immobilized on streptavidin surfaces of IAsys cuvettes, as described under "Experimental Procedures." For each individual concentration of ligate (only data for nSK is shown), the association or binding to immobilized HPG was monitored. Subsequently, the cuvette was washed with binding buffer, and the dissociation phase was monitored (see "Experimental Procedures" for details). For the sake of clarity, only dissociation at saturating ligate concentration is shown. The value of k_{on} for the binding curves for each ligate concentration was determined using the FASTfit™ program, and each value was plotted against the corresponding concentration of the ligate. *Inset*, the plot of k_{on} against ligate concentration for nSK (*filled squares*) or $SK_{del254–262}$ (*open circles*), which gives a *straight line*. The k_a values were obtained from the slope of the *straight line*, and k_d values were calculated from the average of four dissociation curves obtained at saturating ligate concentrations, as described under "Experimental Procedures."

amino-coupling protocol recommended by the manufacturers. The kinetics of association and dissociation of HPG with immobilized nSK/$SK_{del254–262}$ were then measured as described under "Experimental Procedures." In another approach, biotinylated HPG was immobilized on streptavidin captured on a biotin cuvette, and the binding kinetics with SK were studied as described. For these assays, nSK/$SK_{del254–262}$ were added at concentrations ranging between 5 and 80 nM. Relatively fast association kinetics were observed for the binding of both proteins, which is consistent with a monophasic pattern of association (Fig. 2). When the association data for the interaction were fitted to a single exponential curve, a linear relationship was observed between k_{on} and added ligate concentration, according to the equation $k_{on} = k_d + k_a$ (ligate). The results show that the mutant exhibited an affinity that was not significantly different from that of nSK (Table I).

Interestingly, experiments performed by immobilizing nSK/$SK_{del254–262}$ on carboxymethyldextran cuvettes using standard amino-coupling procedures, as shown by other groups also (15, 33), yielded similar binding constants for nSK and $SK_{del254–262}$ (data not shown), indicating that the coupling procedure *per se* does not interfere significantly in the binding interaction between SK and HPG.

To further explore the underlying reason for partial loss of activator activity of the loop deletion mutant, we examined whether, like the native protein, it could expose the active site in partner HPG. For this purpose, we employed the active site acylating agent, NPGB, to test whether the characteristic burst that occurs upon mixing equimolar SK and HPG (3, 25) was also observed with the mutant. Neither SK nor HPG alone give the burst, but only once the two are mixed in equimolar proportions is this burst, characteristically associated with a rapid NPGB hydrolysis, observed due to the formation of a "virgin" SK·HPG complex and consequent acylation at the cryptic active site of HPG with NPGB (3). When the recombinant nSK (used as a control) was tested with this reagent in the presence of equimolar HPG, the characteristic colorimetrically detectable burst was indeed observed. A similar response was evident in the case of $SK_{del254–262}$ as well (Fig. 3, *inset*). However, the maximal level of these bursts was approximately half of that observed with natural SK prepared from *S. equisimilis* (data not shown). It has been demonstrated recently that a free N-terminal residue (Ile) (34) and some flanking residues (35) are required for the auto-activation of HPG by SK. However, the positive NPGB reaction of nSK, albeit less than that of natural SK, was easily explained when N-terminal sequence analysis of

TABLE I

Association and dissociation rate constants and apparent equilibrium dissociation constants for the binding of immobilized HPG to the derivatives of SK

Biotinylated HPG was immobilized on streptavidin captured onto a biotin cuvette. Different concentrations of the nSK/$SK_{del254–262}$ were then titrated as outlined under "Experimental Procedures." The pseudo-first order rate constant (k_{on}) was determined using the FASTfit™ program. The concentration dependence of k_{on} was fitted using linear regression to find the association rate constant (k_a) from the slope of linear fit. The dissociation rate constant (k_d) value was calculated from the average of four dissociation curves obtained at saturating concentration of ligate. The K_D was estimated from the ratio of kinetic constants as k_d/k_a.

Ligate	k_a ($\times 10^6$)	k_d ($\times 10^{-3}$)	K_D ($\times 10^{-9}$)
	$M^{-1}\ s^{-1}$	s^{-1}	M
nSK	1.98 ± 0.08	1.81 ± 0.21	0.91 ± 0.34
$SK_{del254–262}$	1.43 ± 0.07	2.27 ± 0.15	1.58 ± 0.79

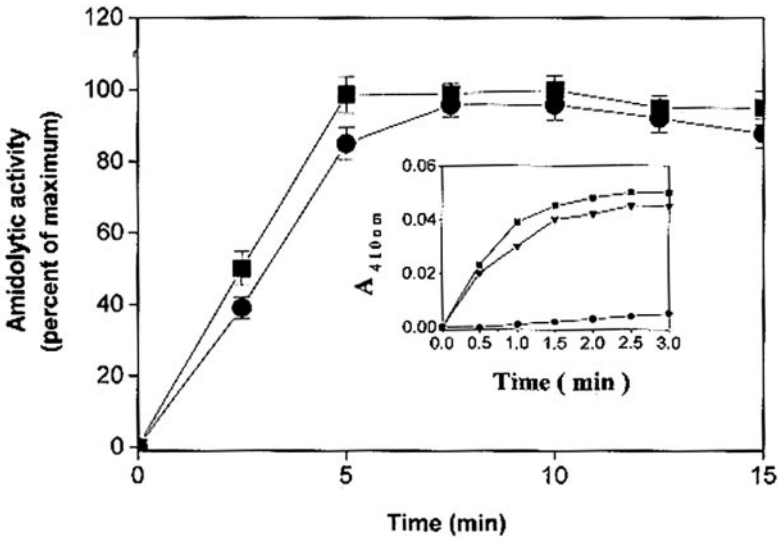

FIG. 3. **Time course of the generation of amidolytic activity of nSK and $SK_{del254-262}$.** Equimolar nSK·HPG and $SK_{del254-262}$·HPG complexes were made, and aliquots were withdrawn at regular periods and transferred into a microcuvette containing 2 mM chromogenic substrate. The generation of amidolytic activity was monitored at 405 nm at 22 °C, as described under "Experimental Procedures." The percentage of maximum amidolytic activity as a function of preincubation time by nSK·HPG complex (*filled squares*) and $SK_{del254-262}$·HPG complex (*filled circles*) is plotted. *Inset*, active site titration of HPG on complexing with nSK or $SK_{del254-262}$ using the active site acylating agent, NPGB. The *figure* shows progress curves of NPGB hydrolysis by nSK·HPG (*filled squares*), $SK_{del254-262}$·HPG (*filled inverted triangles*), and a control reaction (*filled circles*).

the purified nSK and $SK_{del254-262}$ showed that ~50% of the purified protein fractions had (like natural SK) a free Ile at the N terminus, probably due to partial processing by host methionyl aminopeptidase (36). The mutant ($SK_{del254-262}$) was then further verified for its ability to activate partner HPG by carrying out amidolytic assays of its equimolar mixtures with HPG. In this case too, it exhibited a similar, although slightly delayed, time course of generation of amidolytic activity with respect to nSK (Fig. 3), suggesting that it could open the active site in partner HPG. Thus, these results demonstrated that the observed lower HPG activator activity of $SK_{del254-262}$ was not due to any major effect on its ability to activate partner HPG at the binary complex formation stage.

To obtain a glimpse of the functional characteristics of the active site, the kinetic constants associated with the substrate binding and processing of both macromolecular substrate (HPG) and the low molecular weight amidolytic peptide substrate tosyl-glycyl-prolyl-lysine-4-nitranilide acetate were measured by the equimolar complexes of HPN with either nSK or $SK_{del254-262}$. Remarkably, the results for the steady-state kinetic analysis of the activation of substrate HPG by the equimolar $SK_{del254-262}$·HPN complex revealed a 5–6-fold increase in the K_m for HPG when compared with that of nSK·HPN, with relatively little alteration in the k_{cat} values (Table III). This clearly indicated that the loop-deleted mutant formed an activator complex with HPN that had an apparent decreased affinity for the macromolecular substrate as compared with that of the native SK. On the other hand, the k_{cat} values exhibited either by nSK·HPN or $SK_{del254-262}$·HPN for the small MW peptide substrate were essentially unaltered as compared with that of "free" HPN (suggesting that the primary covalent specificity characteristics of the active site in HPN remained unchanged), but, revealingly, the K_m for this substrate was decreased as compared with that of nSK·HPN.

It is known that the complexation of SK with free HPN leads to an overall reduced accessibility of the HPN active site by small molecular weight substrates and inhibitors probably due to steric hindrance brought about by SK binding in the vicinity of the active site; this phenomenon is manifested, for example, in a significant increase in the K_m for the amidolysis of chromogenic substrates by SK·HPN complex compared with that of HPN alone (8, 37, 38). The characteristic increase in K_m of HPN for amidolytic substrates has also been observed with the isolated β domain (11). The present results on the abolition of the "K_m shift" (Table II) in $SK_{del254-262}$ suggest that the 250-loop interacts with a region in partner plasmin(ogen) that is situated close to the active center, a surmise that is entirely consistent with its proposed role in sequestering substrate HPG to the activator complex and with peptide inhibition experiments reported earlier (11). Noticeably, the k_{cat} for the hydrolysis of the low molecular weight peptide substrate by the 1:1 HPN complex of the deletion mutant remained unchanged (Table II). These results clearly demonstrate that the affinity for macromolecular substrate (HPG) was selectively decreased in the case of $SK_{del254-262}$·HPN, without a concomitant alteration in the processivity of the low molecular weight peptide substrate.

The foregoing results on increased K_m for HPG prompted us to explore the comparative affinity of substrate HPG with activator complexes between HPG and nSK, on the one hand, and HPG with $SK_{del254-262}$ on the other, using a more direct physico-chemical approach. For this purpose, a new "docking" assay for ternary complex formation between SK and two mol-

TABLE II
Steady-state kinetic parameters for amidase activity of equimolar complexes of HPN and nSK/$SK_{del254-262}$

For the determination of the amidolytic parameters, nSK/$SK_{del254-262}$ and HPN were precomplexed in an equimolar ratio, and an aliquot of this mixture was assayed for amidolysis at varying concentrations of Chromozym® PL as detailed under "Experimental Procedures." The data represent the mean of three independent determinations.

Protein	K_m	k_{cat}	k_{cat}/K_m
	mM	min^{-1}	min^{-1}/mM
HPN	0.17 ± 0.03	310 ± 18	1823.53
nSK · HPN	0.6 ± 0.02	370 ± 15	616.67
$SK_{del254-262}$ · HPN	0.2 ± 0.07	320 ± 14	1600

TABLE III
Steady-state kinetic parameters for HPG activation by equimolar complexes of HPN and nSK/$SK_{del254-262}$

The kinetic parameters for substrate HPG activation were determined at 22 °C as described under "Experimental Procedures." The data represent the mean of three independent determinations. Closely similar values were obtained for the direct activation of substrate HPG by $SK_{del254-262}$ (data not shown).

Activator protein	K_m	k_{cat}	k_{cat}/K_m
	μM	min^{-1}	$min^{-1}/\mu M$
nSK · HPN	0.5 ± 0.05	11 ± 0.5	22.0
$SK_{del254-262}$ · HPN	2.5 ± 0.3	9.7 ± 0.52	3.9

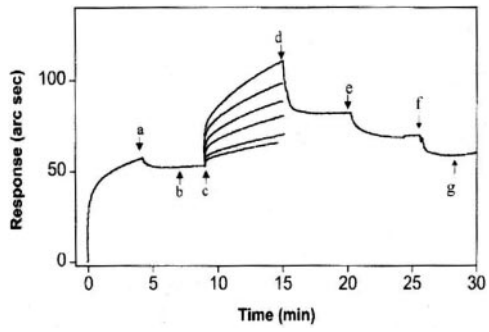

FIG. 4. **Tracings from the IAsys™ resonant mirror-based system to quantitate the interactions between substrate HPG and the equimolar binary complex of nSK and immobilized HPG.** The experiment was carried out at 25 °C in binding buffer as described under "Experimental Procedures." Human PG was biotinylated and immobilized on streptavidin captured onto the biotin cuvette. A stable binary complex was formed by adding saturating concentration of nSK onto immobilized HPG. After washing with binding buffer (point of addition of binding buffer as depicted by *a*), a stable dissociation base line (*b*) was obtained due to high affinity and stability of the SK·HPG binary complex, which remained unaffected even after washing with 2.5 mM EACA (data not shown). Thereafter, varying concentrations of substrate HPG (0.1–1 μM) were then added (point of addition of substrate as depicted by *c* to monitor the association phase (6 min), and subsequently, the cuvette was washed with binding buffer three times (point of addition as depicted by *d*), and the dissociation phase was recorded for the next 6 min. After each cycle of analysis, the undissociated substrate HPG was stripped off with 2.5 mM EACA (point of addition of EACA as shown by *e*), followed by reequilibrating the cuvette with binding buffer (*f*), which reestablished the original base line (*g*). The immobilized streptavidin alone was taken as the negative control, and it was subjected to the same kind of treatments as given to the test cell containing immobilized HPG. No significant nonspecific binding was observed (data not shown).

ecules of HPG, one in the binary mode and the other docked as a substrate, was devised based on a real time approach utilizing resonant mirror-based biosensor equipment (Fig. 4). Earlier, a "static" analysis of the formation of such a ternary complex with radioactively labeled substrate HPG bound onto the binary complex of immobilized HPG and nSK on plastic surfaces has been reported (39). In order to establish the authenticity of ternary complex formation with substrate HPG onto the preformed binary SK·HPG complex on resonant mirror cuvettes, we have used two criteria: (*a*) sensitivity of the ternary complex, and comparative refractoriness of the preformed binary complex, to EACA, and (*b*) distinctive concentration range dependence of binary (low nanomolar range) and ternary complex(es) (high nanomolar range) to HPG binding (see "Experimental Procedures" for detailed protocols). It has been well established that the preformed SK·HPG complex is highly refractory to EACA, whereas the action of the activator complex on the substrate is susceptible to inhibition in the low millimolar range (13), a fact that we also observed, while the same concentration of EACA potently inhibited the interaction of substrate HPG with preformed SK·HPG complex. This comparative resistance of the preformed binary complex and susceptibility of the ternary complex to EACA allowed us to selectively examine the interaction of ternary HPG with the SK·HPG binary complex. Similarly, due to the comparatively low affinity of the substrate HPG toward the SK·HPG binary complex (24), a higher concentration of substrate HPG was required, while the SK-HPG binary interaction, due to its intrinsically high affinity, could easily be monitored at the subnanomolar and low nanomolar ranges of concentration (Tables I and IV).

Ternary interaction studies of HPG with SK·HPG binary complex have been reported earlier using solid phase assay (39). Although such an assay can provide a clear estimate of affinity in terms of equilibrium dissociation constants (K_D), it fails to give insight into the dynamics of the interaction of the activator complex with the macromolecular substrate. The results obtained for the interaction of substrate HPG, μPG, and K1–5 with either nSK or $SK_{del254-262}$ complexed with immobilized HPG are given in Table IV. It is clear that substrate HPG interacts with the $SK_{del254-262}$·HPG binary complex with a 5-fold lower affinity (K_D ~0.75 μM) as compared with nSK·HPG binary complex (K_D ~0.15 μM). This decrease in affinity is remarkably proportionate to the increase in the K_m for substrate HPG (5–6-fold) using enzymatic activity as the criterion for discrimination between nSK and mutant. These results clearly indicate the importance of the 250-loop in "capturing" substrate HPG molecules by the activator complex.

Recent biochemical studies suggest that an exosite-mediated substrate HPG binding, independent of the primary covalent specificity of the HPN active site, represents the major mechanism of SK-induced changes in the macromolecular substrate specificity of HPN (10, 12). The structural basis whereby such an exosite contributes toward the change in substrate specificity of the HPN active site consequent to SK binding has, however, remained essentially unknown so far. The data presented in this paper clearly implicate the 250-loop of the β domain as an important determinant of the macromolecular substrate specificity of the SK·HPG activator complex. The presence of two tandem lysine residues at the tip of the 250-loop suggests that interactions with the kringle domain(s) in substrate HPG may be the operative mechanism behind this interaction. To understand the role of kringles in substrate affinity, the activities of nSK and the mutant were compared in the presence of varying concentrations of EACA, a lysine analogue that is well known to inhibit HPG activation by SK as well as disrupt ternary complex formation through a kringle-mediated mechanism (2, 13, 39). Kinetic studies to check the effect of varying concentrations of EACA on substrate HPG activation by nSK·HPN and $SK_{del254-262}$·HPN showed that the mutant exhibited a greater susceptibility to EACA-mediated inhibition of substrate HPG activation than nSK (Fig. 5*A*) in a concentration range that did not affect the activity of the two binary complexes or the activity of free HPN. It has been shown earlier (13, 39), using a sandwich binding assay, that EACA completely abolishes the docking of substrate HPG onto SK·HPG binary complex formed on a plastic surface. However, this does not allow the measurement of the rates of binding and dissociation of substrate HPG with the high affinity binary complex. Experiments were carried out to see the effect of EACA on the ternary complexation of substrate HPG to nSK/$SK_{del254-262}$ precomplexed with immobilized PG on resonant mirror cuvettes, as described earlier. With $SK_{del254-262}$·HPG binary complex, an IC_{50} of 0.3 mM was obtained, which is ~3-fold less than the IC_{50} (1 mM) obtained with nSK·HPG binary complex (Fig.

TABLE IV

Association and dissociation rate constants and apparent equilibrium dissociation constants for the interaction of substrate HPG, μPG, and K1–5 with nSK/SK$_{del254–262}$ complexed with immobilized HPG

Kinetic constants for the interactions of substrate HPG, μPG, and K1–5 with nSK · HPG or SK$_{del254–262}$ · HPG binary complex were determined by applying the FASTfit™ program to the binding data obtained using IAsys biosensor, as described under "Experimental Procedures." A stable binary complex between nSK/SK$_{del254–262}$ and HPG immobilized onto the cuvette was made, and then the binding of varying concentrations of substrate HPG (0.1–1 μM), μPG (1–6 μM), or K1–5 (1–6 μM) was monitored.

Ligand	Ligate	k_a ($\times 10^5$)	k_d ($\times 10^{-1}$)	K_D ($\times 10^{-6}$)
		$M^{-1}\ s^{-1}$	s^{-1}	M
nSK · HPG	HPG	10.70 ± 1.30	1.76 ± 0.23	0.16 ± 0.04
nSK · HPG	μPG	0.75 ± 0.02	1.29 ± 0.74	1.72 ± 0.91
nSK · HPG	K1–5	0.29 ± 0.06	1.19 ± 0.17	4.11 ± 0.62
SK$_{del254–262}$ · HPG	HPG	4.62 ± 0.51	3.35 ± 0.13	0.72 ± 0.09
SK$_{del254–262}$ · HPG	μPG	0.90 ± 0.03	1.33 ± 0.12	1.48 ± 0.20
SK$_{del254–262}$ · HPG	K1–5	0.28 ± 0.12	3.41 ± 0.21	12.02 ± 2.08

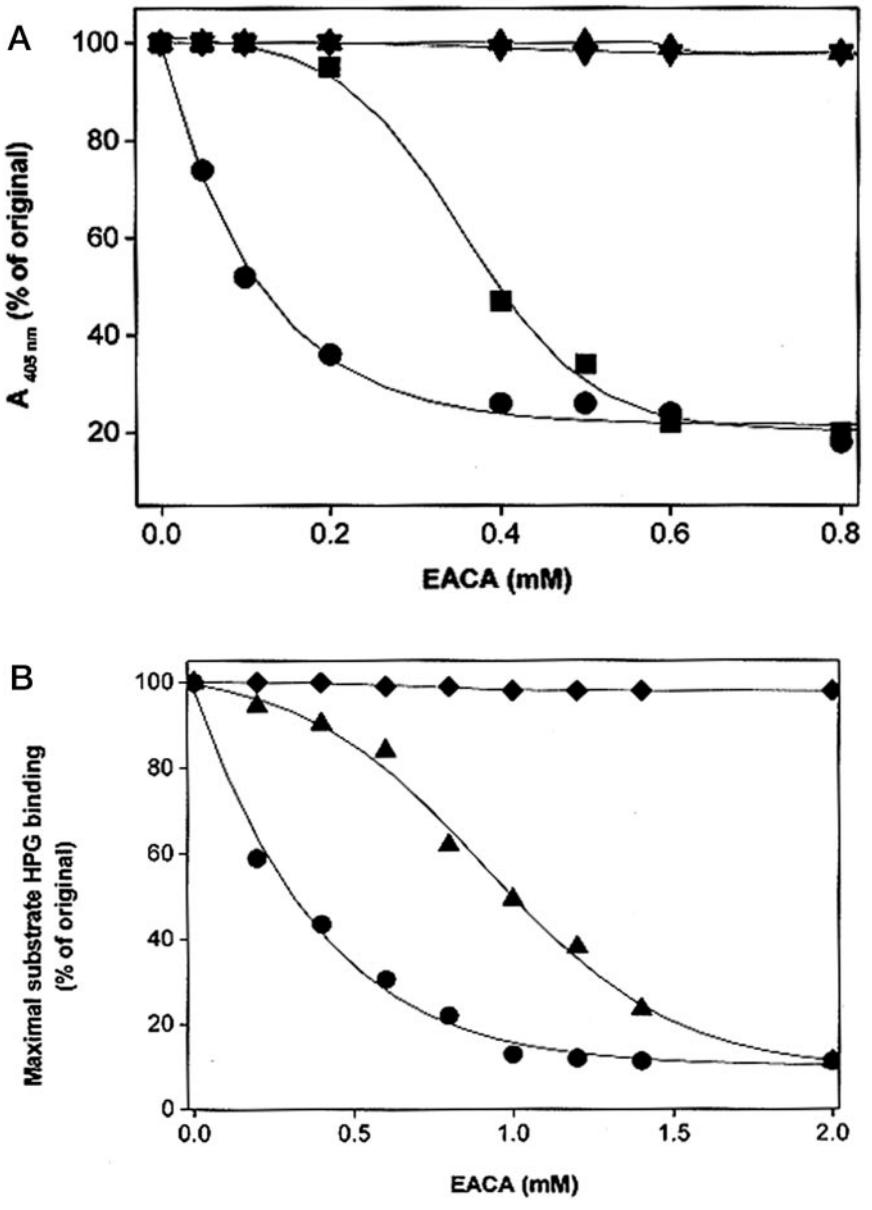

FIG. 5. **Differential susceptibility to EACA of the substrate with binary complexes of nSK and SK$_{del254–262}$-HPG.** *A*, differential susceptibility to EACA of substrate activation by nSK and SK$_{del254–262}$. The effect of different concentrations of EACA (0–1 mM) on the substrate HPG activation by nSK (*filled squares*) and SK$_{del254–262}$ (*filled circles*) was examined. Controls containing a 10 nM concentration each of SK and HPN (*filled triangles*), or HPN alone (*filled inverted triangles*) are also shown. The HPG activator activity of constant, catalytic amounts of the preformed equimolar activator complexes between HPN and either nSK or SK$_{del254–262}$ to obtain final concentrations of 0.25 and 3 nM, respectively in the presence of varying concentrations of EACA, along with substrate HPG and chromogenic substrate in 50 mM Tris-Cl buffer, pH 7.5, was monitored at 405 nm at 22 °C. The initial velocities in different concentrations of EACA are expressed relative to the controls not containing any EACA (taken as 100%). Similar differential effects between nSK and the mutant were observed at HPG concentrations of 0.5, 2, and 4 μM, although the IC_{50} values were different (data not shown). *B*, effect of EACA on the physical binding of substrate HPG to nSK·HPG or SK$_{del254–262}$·HPG binary complex examined by the resonant mirror technique. Binding of substrate HPG (0.4 μM) to either nSK·HPG (*filled triangles*) or SK$_{del254–262}$·HPG

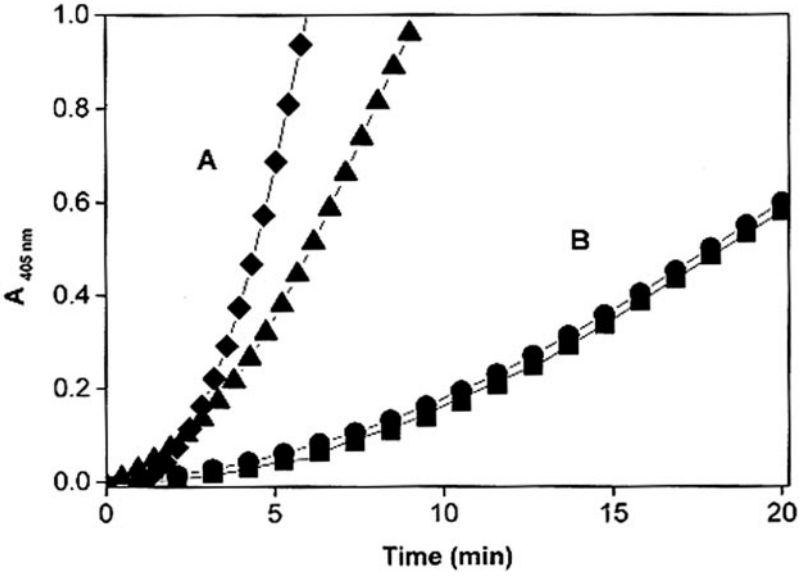

FIG. 6. **Abolishment of the differential substrate activation phenomenon by nSK and $SK_{del254-262}$ by using substrate μPG.** Fixed, catalytic amounts of the respective preformed activator complexes of each protein with HPN were added to the cuvette containing subsaturating concentrations of HPG or μPG as the substrate and Chromozym® PL in 50 mM Tris-Cl buffer, pH 7.5, and the reactions were monitored at 405 nm at 22 °C. The *figure* shows *progress curves* of activation of HPG by nSK (*filled diamonds*) and $SK_{del254-262}$ (*filled triangles*) (*A*) and of μPG by nSK (*filled circles*) and $SK_{del254-262}$ (*filled squares*) (*B*).

5*B*). These data clearly support the conclusion that the binary complex of the mutant, with the 250-loop deleted, interacted with substrate in a manner that is more vulnerable, as compared with nSK-plasmin(ogen), to disruption with the lysine-binding site competitive ligand, EACA. However, it is worth noting that if all of the kringle-mediated interactions between activator and substrate had been abolished by the deletion of the loop, the mutant should have been completely resistant to inhibition by EACA. The fact that the mutant is susceptible to lower concentrations of EACA suggests that other EACA-sensitive kringle-dependent interactions are still operative, but at least one of the critical interactions has been abolished by the selective deletion of the 250-loop.

If the observed difference in substrate affinities between nSK·HPG and $SK_{del254-262}$·HPG activator complexes is indeed kringle-mediated, it is reasonable to assume that the rates of activation of substrate μPG, which is devoid of all five HPG kringles, by nSK and $SK_{del254-262}$ should not substantially differ from each other. This, indeed, was found to be the case (Fig. 6). Microplasminogen is known to be a poor substrate for the preformed SK-PG activator complex (22). Interestingly, kinetic studies using μPG as the substrate showed no discernible difference between nSK and $SK_{del254-262}$ with respect to initial velocities of substrate μPG activation at subsaturating concentrations ($K_m \sim 6 \pm 2$ μM), under conditions where the activator activities of the two complexes (nSK·HPN and $SK_{del254-262}$·HPN) showed a remarkable difference when the substrate (native HPG) contained the kringle domains. These observations prove convincingly that interactions involving lysine binding site(s) in the kringle domains are intimately involved in the mechanism of operation of the macromolecular substrate-specific exosite in the SK-plasmin(ogen) activator complex. To further establish that kringles are involved in activator-substrate interactions, ternary binding experiments on the resonant mirror, where the binding of the substrates, μPG and kringles 1–5 of HPG, to the binary complex preformed between either nSK or the mutant with immobilized HPG, were carried out (Table IV). Remarkably, in consonance with kinetic data, μPG showed the same affinities for both nSK and $SK_{del254-262}$ complexed with HPG. When K1–5 was used as the docking substrate during ternary complex formation, the nSK·HPG binary complex showed an affinity of 4.1 μM for K1–5, while that of the $SK_{del254-262}$·HPG complex was determined to be 12 μM, indicating approximately a 3-fold higher affinity for nSK (Table IV). Again, these results strongly argue that the 250-loop of the β domain of SK interacts with substrate HPG via the latter's kringle domains.

Molecular modeling studies wherein the intermolecular surfaces between the β domain of SK and the isolated kringle 5 (which was used as a typical representative structure of the five HPG kringles and does not necessarily indicate any preferred role in the substrate-activator complex interplay; however, see below) were explored for mutual complementarity (see "Experimental Procedures" for details) indicate that a kringle structure can indeed dock the 250-loop in a remarkably optimal fashion (Fig. 7). Although whether kringle 5 *per se* or any other kringle is involved in this interaction cannot be judged at this stage, during the course of revision of this manuscript, another report was published that demonstrates the involvement of kringle 5 in the 1:1 binding with the β domain of SK (33). Although speculative at this stage, this offers a tantalizing possibility that this kringle-mediated interaction at the levels of both binary and ternary complex formation operates through kringle 5. If this scenario is correct, the loop might switch its binding specificity toward partner or substrate depending on the temporal stage in the catalytic cycle, a possibility that is strengthened by a previous observation (11) that a synthetic peptide encompassing the 250-loop exhibits bifunctional behavior by competitively inhibiting both SK·HPG binding and HPG activation by preformed SK·HPN activator complex. On the other hand, the current evidence does not rule out the possibility that the different kringles in substrate and partner HPG are directed to different sites in SK. Whatever the exact mechanism, this

(*filled circles*) binary complex was measured at various concentrations of EACA (0–2 mM) using the IAsys™ system, as described under "Experimental Procedures." The maximal extent of binding under varying concentrations of EACA was quantitated, and the maximal binding in buffer alone was used to normalize the extent of binding under different experimental conditions. The extent of substrate HPG binding is plotted as a function of EACA concentration. The effect of respective EACA concentrations on the binary nSK/$SK_{del254-262}$·HPG complex is represented by *filled diamonds* (control).

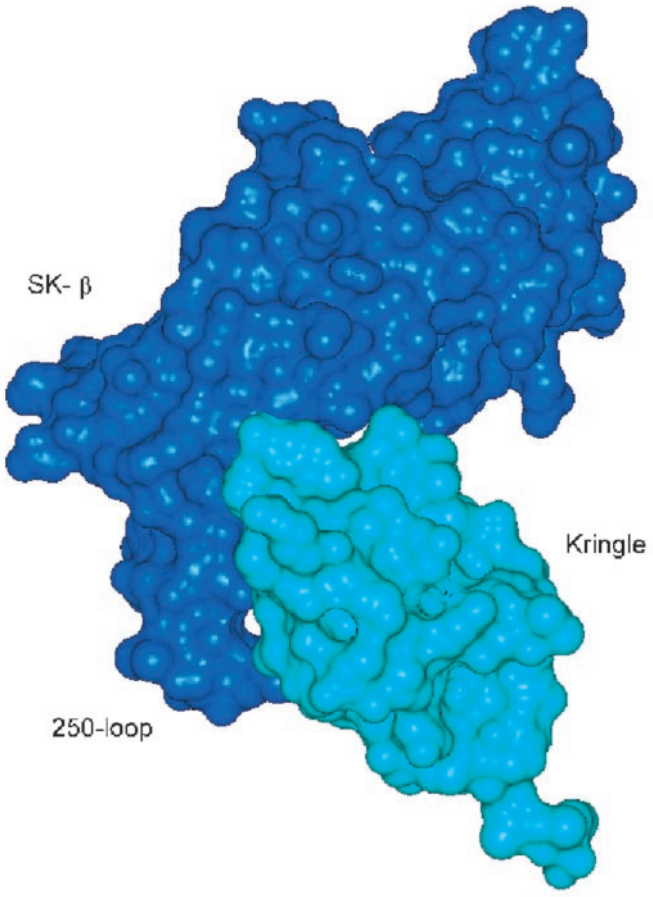

FIG. 7. **Docking of kringle 5 of HPG with the β domain of SK.** Connolly surfaces of the β domain and kringle 5 of HPG were calculated by using the GRASP program. Kringle 5 has been used here as a typical representative structure of the five HPG kringles. In order to generate the molecular surface, the radius of a water molecule was considered to be 1.4 Å. Electrostatic potentials were mapped onto the surfaces with GRASP. The β domain showed a distinct patch of positive charges in the 250-loop. Similarly, the kringle domain also showed a distinct patch of negative charges. The two patches were brought in close proximity by manual docking, which showed close surface and electrostatic complementarities (see "Experimental Procedures" for details).

study provides unmistakable evidence of the direct involvement of a discrete epitope in SK in substrate recognition and binding via the kringle(s) of HPG. Undoubtedly, further studies are needed to identify the relative contributions of the kringle(s) *versus* the catalytic domain of the substrate toward the latter's recognition, docking, and turnover in the "valley" formed by the activator complex. This would aid in a better understanding of this enigmatic interaction at the molecular level.

It must be realized, however, that the observation that, even after the excision of the 250-loop, the HPG activation reaction still survived (albeit with increased K_m) indicates that this loop is not the sole determinant of the SK·HPN exosite property. Indeed, earlier studies had suggested that the α domain as well as the β domain, together, contribute to the generation of HPG specificity in the activator complex (12, 16). The potential of the α domain to interact with substrate HPG is also evident from the SK-μPN crystal structure (8), although whether it does so by interacting with kringle(s) of substrate is still unclear. It is also established from recent work that the β domain contributes a major share toward SK's affinity for partner HPG as well (12). However, the fact that mutagenesis of several residues in the β domain resulted in appreciable diminution in the k_{cat} for activator activity with little change in the K_m for HPG *per se* (16) suggests that regions other than the 250-loop in this domain are also intimately involved in the modulation of the substrate specificity of the activator complex. We have observed[3] that mutations of residues immediately flanking the 250-loop (*e.g.* $SK_{Y252A,E263G}$) lead to further increase in the molecule's K_m for substrate HPG (to about 15-fold that of nSK) with only minimal alteration in the k_{cat} of its complex with HPN.

It is quite intriguing that the β domain provides a major portion of the intermolecular affinity of SK for HPG necessary for the formation of the tightly held equimolar activator complex (15) and at least some of the affinity required for the (transient) interaction of the latter with substrate HPG, as the present study indicates. This arouses curiosity as to whether this domain would, by itself, possess HPG activator activity, however compromised at a quantitative level, since two seemingly fundamental requirements for a single-domain HPG activator protein (*viz*. ability to bind with partner plasmin(ogen) and to then interact with substrate) are present in this domain. This question assumes significance because staphylokinase, a single-domain bacterial HPG activator, is also known to work as a "protein co-factor" in a fashion akin to that of SK (6) and has both of these distinctive HPG interacting properties. The ternary structure of μPN-staphylokinase-μPN suggests that staphylokinase appears not to modify the active site conformation of the enzyme but creates new exosites that indirectly alter the substrate specificity of μPN (40). Identification of such functional "hot spots" in PG activators in general, and SK in particular, that help in exosite-mediated modulation of substrate specificity may greatly aid the future *de novo* design of improved HPG activators.

Acknowledgments—We thank Dr. Amit Ghosh for the facilities provided and support, and Paramjit Kaur for expert technical assistance. We express our gratitude to K. Rajagopal for providing the plasmid construct for the expression of SK $\beta_{wild\ type}$ domain. Automated DNA sequencing was carried out with the unstinted help of Drs. Jagmohan Singh and K. Ganesan. We express our gratitude to Dr. Rajendra P. Roy (National Institute of Immunology, New Delhi) for the use of CD facilities.

REFERENCES

1. International Study of Infarct Survival-3 (1992) *Lancet* **339,** 753–781
2. Castellino, F. J. (1981) *Chem. Rev.* **81,** 431–446
3. McClintock, D. K., and Bell, P. H. (1971) *Biochem. Biophys. Res. Commun.* **43,** 694–702
4. Markus, G., and Werkheiser, W. C. (1964) *J. Biol. Chem.* **239,** 2637–2643
5. Parrado, J., Conejero-Lara, F., Smith, R. A. G., Marshall, J. M., Ponting, C. P., and Dobson, C. M. (1996) *Protein Sci.* **5,** 693–704
6. Esmon, C. T., and Mather, T. (1998) *Nat. Struct. Biol.* **5,** 933–937
7. Conejero-Lara, F., Parrado, J., Azuaga, A. I., Smith, R. A. G., Ponting, C. P., and Dobson, C. M. (1996) *Protein Sci.* **5,** 2583–2591
8. Wang, X., Lin, X., Loy, J. A., Tang, J., and Zhang, X. C. (1998) *Science* **281,** 1662–1665
9. Parry, M. A., Zhang, X. C., and Bode, W. (2000) *Trends Biochem. Sci.* **25,** 53–59
10. Boxrud, P. D., Fay, W. P., and Bock, P. E. (2000) *J. Biol. Chem.* **275,** 14579–14589
11. Nihalani, D., Raghava, G. P. S., and Sahni, G. (1997) *Protein Sci.* **6,** 1284–1292
12. Nihalani, D., Kumar, R., Rajagopal, K., and Sahni, G. (1998) *Protein Sci.* **7,** 637–648
13. Lin, L-F., Houng, A., and Reed, G. L. (2000) *Biochemistry* **39,** 4740–4745
14. Dawson, K. M., Marshall, J. M., Raper, R. H., Gilbert, R. J., and Ponting, C. P. (1994) *Biochemistry* **33,** 12042–12047
15. Conejero-Lara, F. C., Parrado, J., Azuaga, A. I., Dobson, C. M., and Ponting, C. P. (1998) *Protein Sci.* **7,** 2190–2199
16. Chaudhary, A., Vasudha, S., Rajagopal, K., Komath, S. S., Garg, N., Yadav, M., Mande, S. C., and Sahni, G. (1999) *Protein Sci.* **8,** 2791–2805
17. Lin, L-F., Oeun, S., Houng, A., and Reed, G. L. (1996) *Biochemistry* **35,** 16879–16885
18. Wang, X., Tang, J., Hunter, B., and Zhang, X. C. (1999) *FEBS Lett.* **459,** 85–89
19. Deutsch, D. G., and Mertz, E. T. (1970) *Science* **170,** 1095–1096
20. Ho, S. N., Hunt, H. D., Horton, R. M., Pullen, J. K., and Pease, L. R. (1989) *Gene* (*Amst.*) **77,** 51–59
21. Studier, F. W., Rosenberg, A. H., Dunn, J. J., and Dubendorff, J. W. (1990) *Methods Enzymol.* **185,** 60–89
22. Shi, G-Y., and Wu, H-L. (1988) *J. Biol. Chem.* **263,** 17071–17075

[3] J. Dhar and G. Sahni, unpublished observations.

23. Wu, H.-L., Chang, B.-I., Wu, D.-H., Chang, L.-C., Gong, G.-C., Lou, K.-L., and Shi, G.-Y. (1990) *J. Biol. Chem.* **265,** 19658–19664
24. Wohl, R. C., Summaria, L., and Robbins, K. C. (1980) *J. Biol. Chem.* **255,** 2005–2013
25. Chase, T., Jr., and Shaw, E. (1969) *Biochemistry* **8,** 2212–2224
26. Wohl, R. C., Arzadon, L., Summaria, L., and Robbins, K. C. (1977) *J. Biol. Chem.* **252,** 1141–1147
27. Cush, R., Cronin, J. M., Stewart, W. J., Maule, C. H., Molloy, J., and Goddard, N. J. (1993) *Biosensors Bioelectronics* **8,** 347–354
28. Buckle, P. E., Davies, R. J., Kinning, T., Yeung, D., Edwards, P. R., Pollard-Knight, D., and Lowe, C. R. (1993) *Biosensors Bioelectronics* **8,** 355–363
29. Myszka, D. G. (1997) *Curr. Opin. Biotechnol.* **8,** 50–57
30. Morton, T. A., Myszka, D. G., and Chaiken, I. M. (1995) *Anal. Biochem.* **227,** 176–185
31. Radek, J. T., and Castellino, F. J. (1989) *J. Biol. Chem.* **264,** 9915–9922
32. Nicholls, A., Sharp, K. A., and Honig, B. (1991) *Proteins* **11,** 281–296
33. Loy, J. A., Lin, X., Schenone, M., Castellino, F. J., Zhang, X. C., and Tang, J. (2001) *Biochemistry* **40,** 14686–14695
34. Wang, S., Reed, G. L., and Hedstrom, L. (1999) *Biochemistry* **38,** 5232–5240
35. Boxrud, P. D., Verhamme, I. M. A., Fay, W. P., and Bock, P. E. (2001) *J. Biol. Chem.* **276,** 26084–26089
36. Hirel, P. H., Schmitter, J-M., Dessen, P., Fayat, G., and Blanquet, S. (1989) *Proc. Natl. Acad. Sci. U. S. A.* **86,** 8247–8251
37. Robbins, K. C., Summaria, L., and Wohl, R. C. (1981) *Methods Enzymol.* **80,** 379–387
38. Wohl, R. C. (1984) *Biochemistry* **23,** 3799–3804
39. Young, K-C., Shi, G-Y., Wu, D-H., Chang, L-C., Chang, B-I., Ou, C-P., and Wu, H-L. (1998) *J. Biol. Chem.* **273,** 3110–3116
40. Parry, M. A. A., Fernandez-Catala, C., Bergner, A., Huber, R., Hopfner, K-P., Schlott, B., Gührs, K-H., and Bode, W. (1998) *Nature* **5,** 917–923